Design and manufacturing of scanning probe acoustic microscope test phantom

Chen Xiaohui[1], Fang Xiaoyue[1], Song Jitao[2], Ding Mingyue[1,*]

1. Department of Bio-medical Engineering, College of Life Science and Technology, Image Processing and Intelligence Control Key Laboratory of Education Ministry of China, Huazhong University of Science and Technology, Wuhan, Hubei, China, 430074
2. Department of Bio-medical Engineering, College of Life Science and Technology, Britton Chance Center for Bio-medical Photonics at Wuhan National Laboratory for Optoelectronics -Hubei Bioinformatics & Molecular Imaging Key Laboratory, Huazhong University of Science and Technology, Wuhan, Hubei, China,430074

Abstract

Acquiring nondestructive internal structures acoustic image as well as the morphology images using scanning probe acoustic microscope (SPAM) is a challenge and no known metrology tools to identify the ultrasonic internal resolution and detectable depth of SPAM in a nondestructive way. Monitoring these defects necessitates the identification of their technical parameters of SPAM. In this paper, the specific materials (test phantoms) were designed and processed so that the ultrasound internal resolution of SPAM in nondestructive imaging of the embedded or buried substructures as well as the morphology images were measured. Experimental results demonstrated the successful identification of embedded or buried defects under the test phantom with the resolution of 50nm for SPAM as well as the detectable depth of more than 100μm.

Index Terms-Nanomaterials, ultrasound internal resolution, scanning probe acoustic microscope (SPAM).

I.INTRODUCTION

The acquiring the non-destructive internal structure acoustic images as well as morphology images of the materials, components, or biological cells in nanoscale level is critical for the numerous applications in material science, electronics and clinical. Such a new metrology tool is necessary to identify the subsurface defects as well as the topography in a non-destructive way in nanometer scale level. Scanning probe acoustic microscope (SPAM) can be used to acquire non-destructive internal structures acoustic images as well as the morphology images. However, during the process of imaging, the ultrasound internal resolution and detectable depth of SPAM are usually unknown. To verify these parameters, the specific phantoms are needed to be considered as the gold standard to measure them, including the ultrasound internal resolution and maximum detectable depth of the test specimen.

*Ding Mingyue, myding@mail.hust.edu.cn, Department of Bio-medical Engineering, College of Life Science and Technology, Huazhong University of Science and Technology, Wuhan, China, 430074.

Medical Imaging 2015: Ultrasonic Imaging and Tomography, edited by Johan G. Bosch, Neb Duric
Proc. of SPIE Vol. 9419, 94190A · © 2015 SPIE · CCC code: 1605-7422/15/$18
doi: 10.1117/12.2081843

Conventional techniques for imaging buried structures in destructive approaches such as transmission electron microscopy (TEM)[1] usually worked under the vacuum condition. Scanning tunneling microscopy (STM) is nondestructive[2] but can only be used to detect the conductive materials. The conventional approach for detecting buried defects non-destructively is scanning probe microscopy (SPM)[3-5], but it is sensitive only to the surface or subsurface features. Similarly, high-resolution optical microscopy[6-7] is also unable to image the optically opaque or deeply buried structures. Therefore, high resolution imaging of buried structures as well as the morphology is a great challenge and the measurement of the parameters of the technique is inevitable. In addition, most of the imaging resolution of these nondestructive imaging approaches such as optical microscopy[8] are limited by the classical diffraction phenomenon, which makes it difficult to detect the features in nanoscale level.

Scanning probe acoustic microscopy (SPAM) combines the noninvasive penetration nature of ultrasound waves[9] as well as the high-spatial resolution of near-field imaging approach in SPM[10], where a high frequency ultrasound, which provides a high frequency ultrasound signal on the test stage of the machine to detect the buried features, is applied. This signal will vibrate the specimen and produce the motion of the probe on the upper surface of the test specimen. When a laser beam was projected on the surface of the cantilever, the motion of probe is transformed into a motion of spot, which can be captured by a photodiode. This technique offers a nanometer spatial resolution of the topography images as well as the buried defects, and is amenable both for the hard materials such as silicon wafer, soft materials like gel[11], or hybrid structures.

In the scanning probe acoustic microscope, there are many important technical parameters, such as the ultrasound internal ultrasonic resolution and maximum detectable depth. High frequency of SPAM systems can provide a high internal resolution of imaging but failed to pass the deep structure. In our setup, a 2MHz frequency is used for the ultrasound driving and can pass through the specimen more than 100μm.

In this work, the experiments to determine the parameters of our SPAM system were conducted. In this experiment, a gold standard calibration phantom is required to determine the ultrasonic internal resolution and detectable depth of SPAM. Therefore, the design and manufacture of test phantom for this purpose is of great significance in the development of high frequency scanning probe ultrasound microscope system and its application.

On the rest parts of this paper, we first introduce the design and manufacturing of test phantoms, then the method how to test the parameters are given. Finally the experiment as well as their results to measure the parameters of SPAM in nondestructive imaging of the embedded or buried substructures as well as their morphology images are presented.

II. EXPERIMENTAL DETAILS

A. The design and manufacturing of the test phantom

A specimen containing gold nanoparticles buried deep beneath a polymer cover layer was manufactured by dispersing colloidal gold nanoparticles on a silicon wafer substrate with the thickness over 50nm coated with poly(2-vinylpyridine) (PVP). The gold nanoparticles are with the average diameter of 20nm and well dispersed on the PVP film surface. The nanoparticles were then fully covered with 500nm polymer film. Schematic illustration of a nanoparticle phantom is shown as in Fig. 1.

B. Test phantom validation

• Experimental apparatus and materials

(1) CSPM5500, an open scanning probe acoustic microscope, from Being Nano-Instruments Ltd, Guangzhou, China, was used as the measurement platform.

(2) The silicon wafer phantom with nanoparticles. A silicon wafer consisting of gold nanoparticles buried deep beneath a polymer cover layer was manufactured by dispersing colloidal gold nanoparticles on a silicon wafer substrate coated with poly(2-vinylpyridine) (PVP).

(3) The silicon wafer phantom without nanoparticles. A silicon wafer consisting of a polymer cover layer on a silicon wafer substrate coated with poly without any gold nanoparticles.

(4) Coupling agent. Coupling with normal ultrasound coupling agent, makes the specimen contact with the test stage closely.

(5) Contact probe. A specific type of probe, contact probe is used for the scan. The probe is touched with the surface of the phantom that no buried the gold nanoparticles existed so that the acoustic image is shown the internal structure information of the specimen passing through it.

(6) Ultrasound transducer. The 2MHz ultrasound transducer is used to provide the ultrasound signal on the test stage, i.e., beneath the specimen.

• Experimental method

(1) Installation of the contact probe

Load the contact probe carefully with the tweezers into the cantilever holder of SPAM according to the operation instructions. It is necessary to clean the cantilever holder with ethanol before the experiments, which helps to limit the contamination during the AFM measurement[12].

(2) Specimen loading

Place the specimen on the SPAM stage and ensure it well contacted using the ultrasound coupling agent; then engage the contact probe tip on the middle of the specimen. It is important to guarantee that the whole experiment was performed in a quiet environment.

(3) Images acquisition

Collect the acoustic images and morphology images by scanning the test phantoms. Move the phantom left and collect the acoustic images and morphology images again by scanning the same phantom.

(4) Images analysis

Analyze the acoustic images and morphology images of the test phantoms with the software in the system, respectively. Then analyze the acoustic images of the two phantoms in the corresponding position.

III. RESULTS AND DISCUSSIONS

Analysis on the collected images was implemented on the CSPM5500 SPAM system, and the results were achieved by testing the method with the designed test phantoms. Some black holes were observed in the acoustic images by scanning the test phantom with the nanoparticles while no such holes were observed in the test phantom without the nanoparticles. For the test phantom, no the similar black holes are found in the corresponding positions of the morphology image of the same phantom. This is further demonstrated by moving the phantom where the black holes are moved with the same motion of the phantom. The same phenomenon can be observed after moving the phantom to the left. After measuring by the on-board software, the diameter of the black hole is more than 100 nm.

Figures 2 and 3 showed the acoustic images and their morphology images acquired by scanning a test phantom without and with the nanoparticles respectively. Figure 4 showed the acoustic images and morphology images obtained by scanning the test phantom with the nanoparticles when it was moved to the left. Figures 5 showed the morphology image of TGZ02 standard phantom (as shown in Fig. 8). As shown in Fig. 5, 34 strips are observed in the image and the horizon range between two adjacent strips is 3109.84nm. Thus, the largest scanning size of our system is more than 100μm*100μm.

Figure 6 showed the morphology of a mica specimen and the crystal lattice of the mica were visible in the image and Fig. 7 is the morphology image of the mica after Fourier transform processing with the on-board software. It can be measured that the crystal lattice of the mica specimen is 0.52nm in the profile analysis diagram.

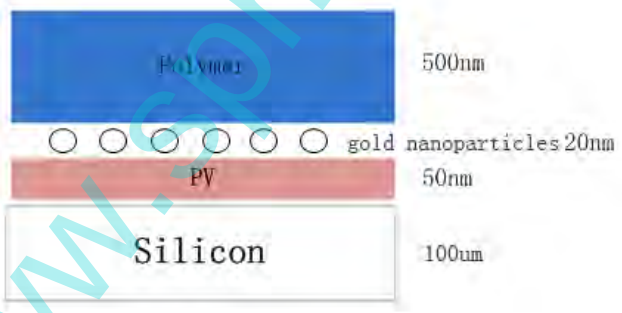

Fig. 1.Schematic illustration of a nanoparticle phantom for validation of our SPAM system. The gold nanoparticles were dispersed on a polymercoated substrate (PV) buried under a 500nm thick polymer layer and the thick of the silicon wafer is about 100μm .

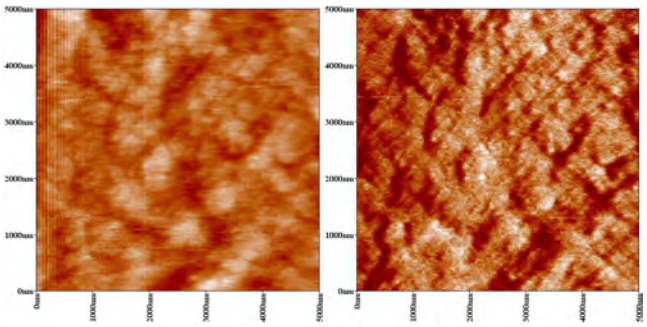

Fig. 2.The morphology image (left) and acoustic image (right) of the silicon wafer phantom without nanoparticles (a specimen consisting of a polymer cover layer on a silicon wafer substrate coated with poly)

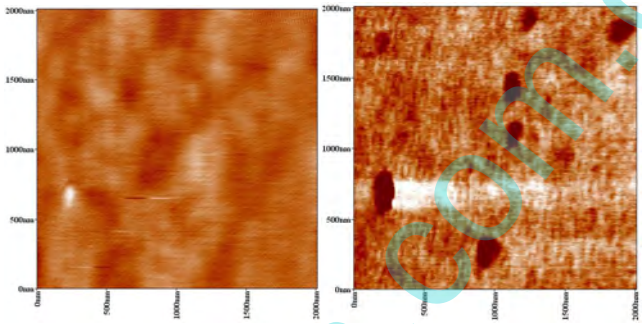

Fig. 3.The morphology image (left) and acoustic image (right) of the silicon wafer phantom with nanoparticle (a specimen consisting of gold nanoparticles buried deep beneath a polymer cover layer was prepared by dispersing colloidal gold nanoparticles on a silicon wafer substrate coated with poly)

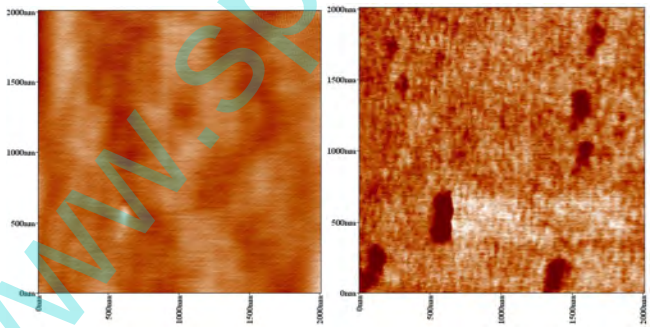

Fig. 4.The morphology image (left) and acoustic image (right) of the silicon wafer phantom with the nanoparticles after it was moved to the left.

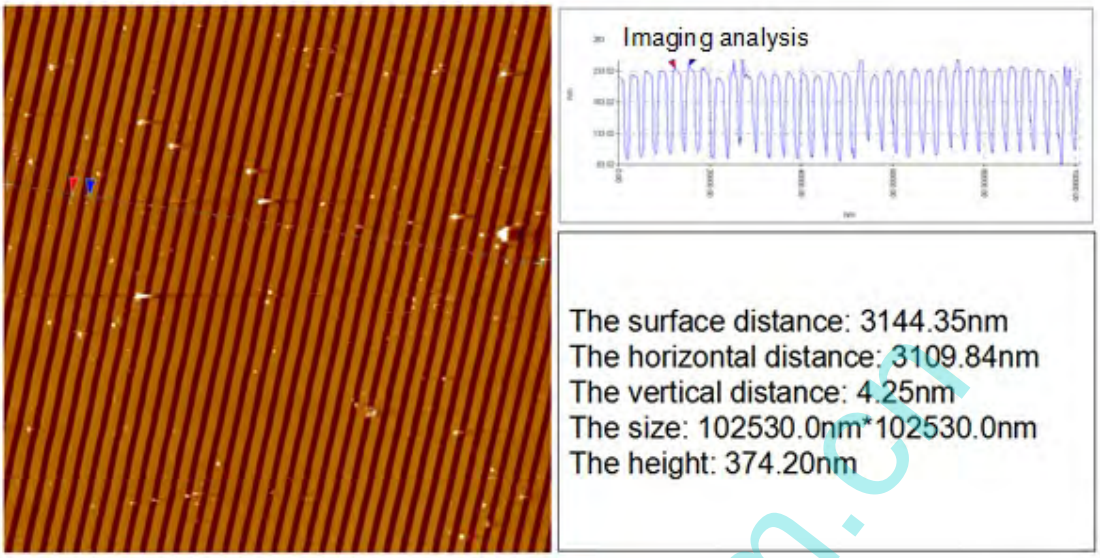

Fig. 5.The morphology image of the specific standard phantom TGZ02.

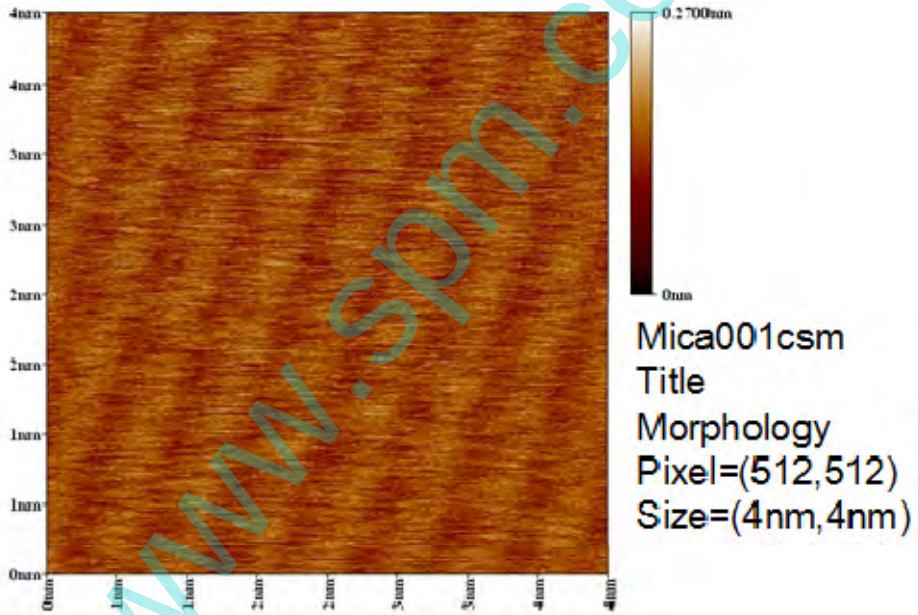

Fig. 6.The morphology image of a mica wafer.

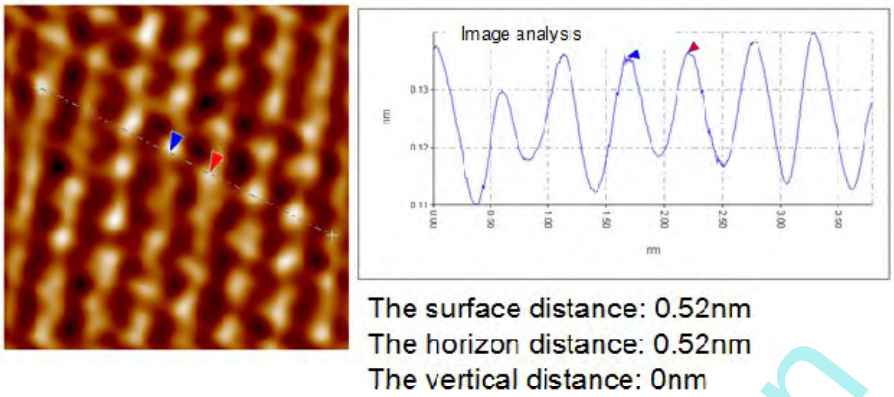

Fig. 7.The morphology image of the mica after Fourier transform and the profile analysis diagram of the image.

Fig. 8The standard phantom TGZ02 for the scanning size measurement

IV. CONCLUSION

Since the acoustic property of silicon wafer is different from that of gold nanoparticles and the phantom acoustic wave is perturbed by the buried features, which can react the difference in the acoustic images when the ultrasound wave penetrates the test phantom.

The experimental results demonstrated the acoustic images by scanning the silicon wafer phantom can obtain more details than the morphology image of the same phantom. The ups and downs of silicon wafer phantom does not cause the emergence of the black holes with the diameter of 100 nm, thus, we came the preliminary conclusion that the ultrasonic internal resolution of SPAM was under 100 nm. The scanning size of the SPAM is more than 100μm*100μm measured by the specific standard phantom of TGZ02 and the lateral resolution of the SPAM is less than 0.52nm in morphology image because the crystal lattice of the mica phantom is distinguishable using the SPAM .The proposed method is used for accurately verifying the ultrasonic internal resolution of the SPAM if the high-frequency ultrasound wave is launched both from the test stage and the SPAM cantilever simultaneously, which is one of our future works.

ACKNOWLEDGMENTS

The authors would like to thank Guangzhou Being Nano-Instruments Ltd for providing the open SPM platform CSPM5500 for our setup. This work was sponsored by The major national scientific instrument and equipment development project under the grant No. 2013YQ160551.

REFERENCES

1. Kunze U. Invited Review Nanoscale devices fabricated by dynamic ploughing with an atomic force microscope[J]. Superlattices and microstructures, 2002, 31(1): 3-17.
2. Chen C H, Deen M J. A general procedure for high-frequency noise parameter de-embedding of MOSFETs by taking the capacitive effects of metal interconnections into account[C]//Microelectronic Test Structures, 2001. ICMTS 2001. Proceedings of the 2001 International Conference on. IEEE, 2001: 109-114..
3. Somekh M G, Bertoni H L, Briggs G A D, et al. A two-dimensional imaging theory of surface discontinuities with the scanning acoustic microscope[J]. Proceedings of the Royal Society of London. A. Mathematical and Physical Sciences, 1985, 401(1820): 29-51.
4. Binnig G, Gerber C, Stoll E, et al. Atomic resolution with atomic force microscope[J]. EPL (Europhysics Letters), 1987, 3(12): 1281.
5. Twerdowski E, von Buttlar M, Razek N, et al. Combined surface-focused acoustic microscopy in transmission and scanning ultrasonic holography[J]. Ultrasonics, 2006, 44: e1301-e1305.
6. Dickson W, Takahashi S, Pollard R, et al. High-resolution optical imaging of magnetic-domain structures[J]. Nanotechnology, IEEE Transactions on, 2005, 4(2): 229-237.
7. Denyer M, Micheletto R, Nakajima K, et al. Biological imaging with a near-field optical setup[J]. Journal of nanoscience and nanotechnology, 2003, 3(6): 496-502.
8. Shekhawat G S, Avasthy S, Srivastava A K, et al. Probing buried defects in extreme ultraviolet multilayer blanks using ultrasound holography[J]. Nanotechnology, IEEE Transactions on, 2010, 9(6): 671-674.
9. Shekhawat G, Srivastava A, Avasthy S, et al. Ultrasound holography for noninvasive imaging of buried defects and interfaces for advanced interconnect architectures[J]. Applied physics letters, 2009, 95(26): 263101.
10. Shekhawat G S, Dravid V P. Nanoscale imaging of buried structures via scanning near-field ultrasound holography[J]. Science, 2005, 310(5745): 89-92.
11. Shekhawat G S, Chand A, Sharma S, et al. High resolution atomic force microscopy imaging of molecular self assembly in liquids using thermal drift corrected cantilevers[J]. Applied Physics Letters, 2009, 95(23): 233114.
12. Thomas G, Burnham N A, Camesano T A, et al. Measuring the mechanical properties of living cells using atomic force microscopy[J]. JoVE (Journal of Visualized Experiments), 2013 (76): e50497-e50497.